VOL. 294 NO. 8 AUGUST 2011

The Anatomical Record

Advances in Integrative Anatomy and Evolutionary Biology

Celebrating
OVER 100 YEARS
of Excellence in
ANATOMICAL PUBLICATION

THE ANATOMICAL RECORD AUGUST 2011 VOL. 294-NO. 8-PAGES 1273-1432 WILEY-BLACKWELL
AN OFFICIAL PUBLICATION OF THE AMERICAN ASSOCIATION OF ANATOMISTS KURT H. ALBERTINE • EDITOR-IN-CHIEF

Convergent Evolution Driven by Similar Feeding Mechanics in Balaenopterid Whales and Pelicans

DANIEL J. FIELD,[1,2]* SHENG CHUAN LIN,[2] MICHA BEN-ZVI,[2] JEREMY A. GOLDBOGEN,[3] AND ROBERT E. SHADWICK[2]

[1]Department of Geology and Geophysics, Yale University, 210 Whitney Avenue, New Haven, Connecticut

[2]Department of Zoology, University of British Columbia, 6270 University Boulevard, Vancouver, British Columbia, Canada

[3]Cascadia Research Collective 218 1/2 W 4th Avenue, Olympia, Washington, USA

ABSTRACT

The feeding apparatuses of rorqual whales and pelicans exhibit a number of similarities, including long, kinetic jaws that increase gape size, and extensible tissue comprising the floor of the mouth. These specializations enable the engulfment of large volumes of prey-laden water in both taxa. However, the mechanics of engulfment feeding in rorquals and pelicans have never been quantitatively compared. Here, we use "BendCT," a novel analytical program, to investigate the mechanical design of rorqual and pelican mandibles, to understand whether these bones show comparable designs for resisting similar hydrodynamical loads. We also compare the mechanical properties of the extensible tissue used during engulfment in rorquals and pelicans. We demonstrate that the evolutionary convergence in the feeding apparatus of rorquals and pelicans is more pronounced than has been recognized previously; both taxa exhibit mandibular flexural rigidity distributions suited for resisting dorsoventral bending stresses encountered while feeding, and possess similarly extensible tissue on the floor of their mouths. Anat Rec, 294:1273–1282, 2011. © 2011 Wiley-Liss, Inc.

Key words: rorqual; pelican; flexural rigidity; convergence

The extraordinary engulfment feeding behaviors of rorqual whales (Balaenopteridae) and Brown Pelicans (*Pelecanus occidentalis*) bear numerous similarities (Brodie, 2001). Both groups exhibit edentulous mandibles that comprise approximately 25% of total body length, as well as highly extensible tissue comprising the floor of their mouths (Brodie, 2001). This tissue is known as ventral groove blubber (VGB) in rorquals, and gular sac tissue in pelicans. When feeding, rorquals depress their mandibles up to 80° while swimming at speed under water, and Brown Pelicans plunge into water headfirst from up to 16 m and depress their mandibles soon after impact (Allen, 1923; Schreiber et al., 1975). VGB and gular pouch tissue facilitate the engulfment of large volumes of prey-laden water relative to body size in both groups: Brodie (2001) predicted that the dynamic inflation of this extensible tissue during engulfment feeding may increase a whale's total body volume by 50%, and may increase a Brown Pelican's volume by as much as 250%. Although the general similarities between pelican and rorqual feeding are clear (Fig. 1), a comparison of feeding mechanics in these taxa has never been performed. This has prevented the assessment of whether the apparent similarity of the feeding apparatus in these groups has been driven by similar feeding mechanics, and has obscured the degree to which these taxa have converged morphologically. Here, we present the first

Grant sponsor: NSERC USRA (DJF) and NSERC Discovery Grant (RES).

*Correspondence to: Daniel J. Field, Department of Geology and Geophysics, Yale University, 210 Whitney Avenue, New Haven, Connecticut 06511. Fax: 203 432-3980.
E-mail: daniel.field@yale.edu

Received 18 January 2011; Accepted 18 March 2011

DOI 10.1002/ar.21406
Published online 25 May 2011 in Wiley Online Library (wileyonlinelibrary.com).

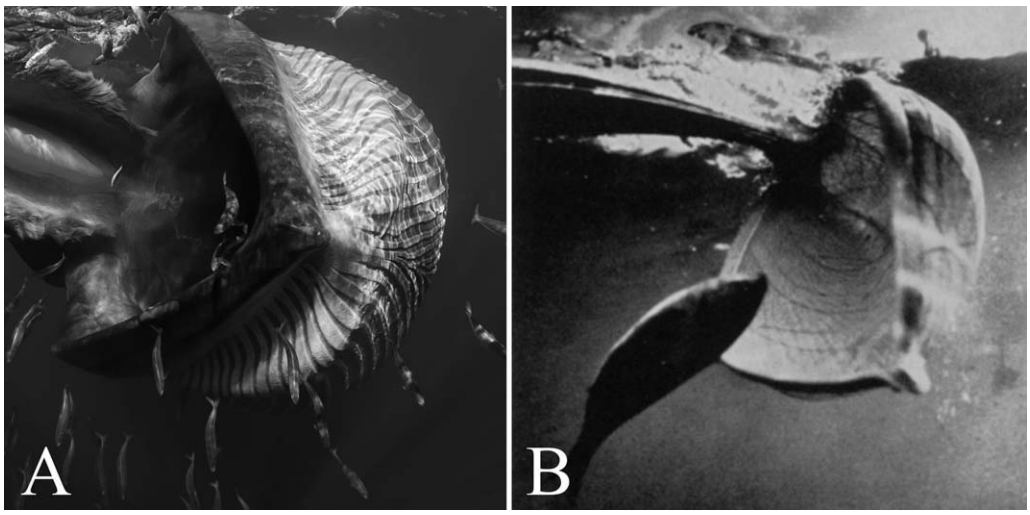

Fig. 1. Action shots of engulfment feeding in a Bryde's whale (**A**) and a Brown Pelican (**B**). Morphological similarities such as elongated rostrums, large gape sizes and extensible tissue comprising the floors of the mouths are visible. Bryde's whale photo courtesy of Doug Perrine (www.seapics.com); pelican photograph modified from Schreiber et al. (1975), use courtesy of The Auk and The American Ornithologists' Union.

quantitative comparison of mandibular architecture in rorquals and pelicans, to assess mechanical similarity in their feeding habits.

Field et al. (2010) used quantitative computed tomography to investigate the mechanical properties of humpback whale (*Megaptera novaeangliae*) mandibles. This study suggested that rorqual mandibles exhibit a mechanical design (density and shape distribution) that is ideally suited to resisting strong dorsoventral bending stresses during a feeding event. When a Brown Pelican dives into the water from a height of 4 to 16 m and opens its mouth, the rapid inflation of its gular pouch may also exert substantial dorsoventral bending stresses on the mandibles. The breakage of a pelican's lower jaw during feeding would lead to the bird's eventual starvation in the wild; therefore, if strong bending stresses are encountered by Brown Pelican jaws, their mandibles should exhibit a design that is similar to that observed in rorquals (McSweeney and Stoskopf, 1989).

Stress in a uniformly loaded cantilever beam is maximal at the beam's fixed end, and decreases to zero at its free end. Therefore, an optimal design for resisting uniform dorsoventral bending stresses would involve an increase in flexural rigidity (a measure of bending stiffness) from the front (rostral) end of the mandible to the back (caudal) end, up to the point that the jaw is anchored to the skull (Bock, 1968; Vogel, 2003). We hypothesized that the mechanics of engulfment feeding in pelicans and rorquals are both characterized by exposure of the mandibles to extreme dorsoventral bending stresses; therefore, we predicted that rorqual and Brown Pelican mandibles should both exhibit increasing trends in mandibular flexural rigidity from their rostral ends to the point that they become constrained by jaw musculature and the craniomandibular joint (Field et al., 2010). A visual juxtaposition of rorqual and pelican mandibles is provided in Fig. 2.

For comparison, we analyzed mandibular flexural rigidity trends in the American White Pelican (*Pelecanus erythrorhynchos*) and the Double-crested Cormorant (*Phalacrocorax auritus*), in addition to analyzing the caudorostral trends in flexural rigidity for rorqual and Brown Pelican mandibles. Cormorants are seabirds that may be distantly related to pelicans (Hackett et al., 2008), and snatch fish out of the water column with their beaks (Owre, 1967). American White Pelicans scoop mouthfuls of prey-laden water from the upper 1.25 m of the water column while floating on the water's surface (Anderson, 1991). The feeding method of American White Pelicans may expose their mandibles to moderate amounts of bending, and that of the cormorant should not expose their mandibles to significant bending stresses. Therefore, we predicted similar flexural rigidity trends in the mandibles of the American White Pelican and the Brown Pelican, but with lower actual flexural rigidity values in the American White Pelican. We predicted that the flexural rigidity trends in the cormorant would be unrelated to those in pelicans or rorquals.

Both rorquals and pelicans have mechanisms for increasing gape size beyond simply depressing their mandibles. Rorqual mandibles roll laterally and move outward during a feeding lunge such that their gape exceeds the width of their rostrum—actions referred to as alpha and omega rotation, respectively (Lambertsen et al., 1995). Pelicans, by contrast, exhibit "streptognathism": the ability to actively bow their mandibles outward by contraction of the pterygoideus musculature (Böker, 1934; Judin, 1961; Burton, 1977; Meyers and Myers, 2005). This bending occurs in the mediolateral plane, and the mechanics underlying this action have been discussed before (Judin, 1961; Meyers and Myers, 2005). To our knowledge, however, the pelican mandible's ability to resist bending in the dorsoventral plane has never been investigated. This element of mandibular design may be critical for resisting jaw fracture during feeding.

Orton and Brodie (1987) discussed the elastic properties of rorqual VGB, but the mechanical properties of the pelican gular pouch have not been examined. Here, we present the first data on the material properties of

Brown Pelican gular pouch tissue, as well as the relative bending resistance of the Brown Pelican mandible in dorsoventral and mediolateral orientations.

MATERIALS AND METHODS

Dried and degreased mandibles from a subadult humpback whale (*Megaptera novaeangliae*), adult minke whale (*Balaenoptera acutorostrata*), American White Pelican (*Pelecanus erythrorhynchos*), Brown Pelican (*Pelecanus occidentalis*), and Double-crested Cormorant (*Phalacrocorax auritus*), obtained from the zoological collections of the Cowan Vertebrate Museum at the University of British Columbia, were scanned alongside hydroxyapatite rods of known density at a high-resolution CT scanning facility. Posteroanterior chord lengths were obtained for each of the bones studied, and these measurements are presented in Table 1. Slice thicknesses of 1 cm were obtained for the humpback and minke whale mandibles, and all of the bird mandibles were scanned at a slice thickness of 0.082 mm. All of the data were saved in stacks of high-resolution DICOM files. Every 35th bird jaw image was analyzed, resulting in a between-slice thickness of 2.86 mm, and every whale mandible slice was analyzed. These resolutions were sufficient to observe small-scale differences in flexural rigidity from one slice to the next.

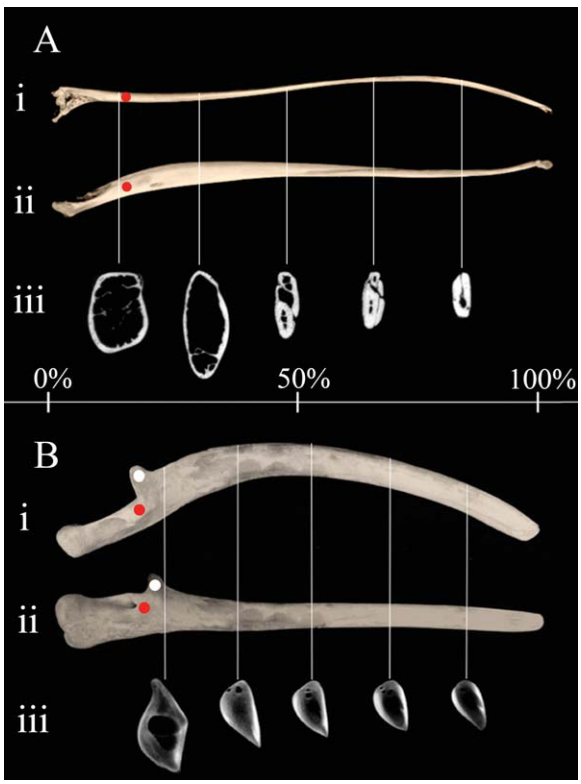

Fig. 2. Dorsal (i), Medial (ii), and cross-sectional (iii) views of the left mandible of a Brown Pelican (**A**) and a minke whale (**B**). Percent distance from the posterior end of the mandibles is indicated in the middle of the figure. In photographs (i) and (ii) posterior is to the left, and anterior is to the right. In the cross-sections (iii), lateral is left, medial is right, dorsal is up and ventral is down. Red dots denote the anterior extent of the posterior jaw constraints. White dots in (B) denote the coronoid process of the mandible.

The densities of the hydroxyapatite standards used in this study are based on the amount of calcium hydroxyapatite suspended in water-equivalent resin when the standards were manufactured (Campbell-Malone, 2007). We used least squares to determine the relationship between Hounsfield units (reported by our laboratory imaging software), and bone density (ρ), reported in g/cc.

Maximum engulfment capacity of an adult male Brown Pelican was determined by gradually filling the pouch with a large graduated cylinder filled with dry rice, and the pelican's body volume was determined using Archimedes' principle. This enabled an estimation of the extent to which a pelican's volume may increase during an engulfment-feeding event.

We used engineering beam theory to analyze the mechanical properties of the mandibles. Flexural rigidity is the product of an object's elastic stiffness, quantified as the Young's modulus (E), and its cross-sectional shape, quantified as the second moment of area (I):

$$\text{Flexural Rigidity} = E(I) = E\int_A y^2(dA) \qquad (1)$$

where y is the distance between the area increment dA and the bending axis of interest. Although an average value of E can easily be estimated from CT scan data (see Field et al., 2010), EI, using average values, does not yield a particularly useful result, as it does not take into account the possibility of nonhomogeneity in cross-sectional mineral density, which leads to regional variation in E. Therefore, we generated a MATLAB script (dubbed "BendCT") to compute cross-sectional flexural rigidity on a pixel-by-pixel basis for each slice, using a similar algorithm to that proposed by Hong et al. (2003). This was done by defining dA as the area of a pixel and taking the summation form of the integral as follows:

$$\sum_{i=1}^{n} E_i(y_i^2)dA_i \qquad (2)$$

where i identifies an individual pixel, and n is the total number of pixels in the user defined region of interest.

TABLE 1. Maturity data and posteroanterior chord lengths of the mandibles examined in this study

Species	Chord length of mandible (cm)	Maturity
Humpback whale (*Megaptera novaeangliae*)	207.4	Weaned sub-adult
Minke Whale (*Balaenoptera acutorostrata*)	143.3	Adult
Brown Pelican (*Pelecanus occidentalis*)	36.2	Adult
White Pelican (*Pelecanus erythrorhynchos*)	35.0	Adult
Double-crested cormorant (*Phalacrocorax auritus*)	10.4	Adult

Specimens measured according to method presented by Field et al. (2010).

In this way, BendCT allowed for the calculation of flexural rigidity weighted by the effect of bone density on E, relative to a user-defined axis of bending.

CT cross-sections for each specimen were imported into BendCT at the aforementioned slice thicknesses. The dorsoventral axis of each bone was determined, and this axis was selected for analysis in each stack of cross-sections. The reported value of flexural rigidity for each slice was determined about this axis, and the program reported flexural rigidity in units of Nm^2.

Using a dataset of human cancellous bone loaded in compression along its vertical axis, Rice et al. (1988) derived an equation for estimating Young's modulus (E, in MPa), from density (ρ in g/cc). Campbell-Malone (2007) verified that this equation provided an accurate estimation of E for right whale mandibles. Therefore, we used this equation to determine E from our QCT-derived values of apparent density (ρ_{app}):

$$E = 1000 \times [0.07 + 0.82(\rho_{app})^2] \quad (3)$$

To determine if rorqual and Brown Pelican mandibles were optimized for resistance to dorsoventral bending, we used BendCT to determine the value of EI along the dorsoventral axis of each CT slice, and to determine the maximum possible value of EI in any orientation through each slice. Discrepancies between the dorsoventral EI magnitude and the maximum possible EI magnitude were interpreted as evidence of a given slice not exhibiting optimality for dorsoventral bending resistance.

To establish an informative comparison between the flexural rigidity trends in whale and Brown Pelican jaws, adjusted EI values were calculated by scaling the cross-sectional area (including spaces within the bone) of Brown Pelican mandible slices to match those of the humpback whale jaw slices at equivalent positions, using eq. 4. With the assumption that the Young's modulus of bone remained constant during scaling, the EI value of the resultant "whale-sized" pelican jaw slices could be determined by adjusting for an increased I due to increased cross-sectional area:

$$EI_{\text{pelican adjusted}} = (A_{\text{whale}}/A_{\text{pelican}})^2 * EI_{\text{pelican}} \quad (4)$$

where A denotes the cross-sectional area of the jaw at a given point along its length.

Biaxial stress versus strain curves were created for Brown Pelican gular pouch tissue according to the methods of Charalambides et al. (2002). As well, the increase in stiffness of the Brown Pelican mandible in the dorsoventral plane relative to the mediolateral plane was estimated by taking the ratio of mandibular deflection in the dorsoventral plane to deflection in the mediolateral plane, for equivalent masses added to the rostral tip of a clamped mandible, in both orientations.

A circular sample taken from the central region of the Brown Pelican gular pouch was mounted between two circular metal disks, with an aperture of 5 cm, on a water-pressurized chamber to achieve biaxial bubble inflation (Reuge et al., 2001). Two digital cameras were set up to capture the top and side views of the pelican pouch being inflated at different pressures. From these images, the half chord length and height of the bubble were measured from the top and side images, respectively. The radius of curvature, r, was then determined:

$$r = (\text{halfchord})/\sin(2 \bullet \tan^{-1}(\text{halfchord}/\text{height})) \quad (5)$$

Nominal stress, σ, at the pole of the bubble was then calculated using eq. 6 (Murphy et al., 2005):

$$\sigma = p \cdot (r/2t) \quad (6)$$

where p is pressure and t is the initial thickness of the pelican pouch. Stresses were calculated in both the long and short axis of the bubble, corresponding to the transverse and longitudinal direction of the pouch *in vivo*, respectively. Two samples of tissue were tested in this manner. Strain ($\varepsilon = \Delta L/L_o$) in each of the long and short axes was measured from the top view images.

RESULTS

The caudorostral flexural rigidity trends for all five species examined are depicted in Fig. 3. This figure illustrates that, throughout most of the jaw, the flexural rigidity of the Brown Pelican mandible is greater than that of the American White Pelican, and that both pelican species have higher flexural rigidity values than the cormorant. The flexural rigidity of the whale mandibles increases steadily from the rostral to the caudal end of the mandible, before decreasing where the mandible is constrained by TMJ pads. The same is true for the trends through the American White Pelican mandible (increasing posteriorly before decreasing through the mandibular condyle); however, maximum flexural rigidity occurs anterior to the mandibular condyles in the Brown Pelican and cormorant mandibles. The two peaks in flexural rigidity anterior of the TMJ in the subadult humpback mandible are due to low mineralization through the coronoid process (high EI immediately anterior and posterior of the process). Field et al. (2010) predicted that adult rorqual mandibles would show no such decrease through the coronoid process; indeed, the adult minke whale mandibles show a highly mineralized coronoid, and a correspondingly high value of flexural rigidity in that region.

Figure 4 depicts the results of mathematically scaling Brown Pelican mandibles up to the dimensions of humpback whale mandibles. These results show that, for their size, the mandibles of the Brown Pelican are more resistant to bending than the humpback whale mandible. The difference becomes more pronounced anteriorly, where the humpback mandible becomes less optimized for dorsoventral bending resistance.

Figure 5 displays the ratio of flexural rigidity oriented along a mandible's dorsoventral axis to the maximum possible value of EI for a given cross-section. For the Brown Pelican, the close adherence of this value to 1 indicates that the bone is well designed for dorsoventral bending resistance along its length; however, for the humpback whale, the deviation from 1 in the rostral portion of the mandible suggests that mandibular morphology at this point resists loads other than dorsoventral bending, such as torsion.

Figure 6 depicts load versus deflection curves for a Brown Pelican mandible loaded in the dorsoventral and

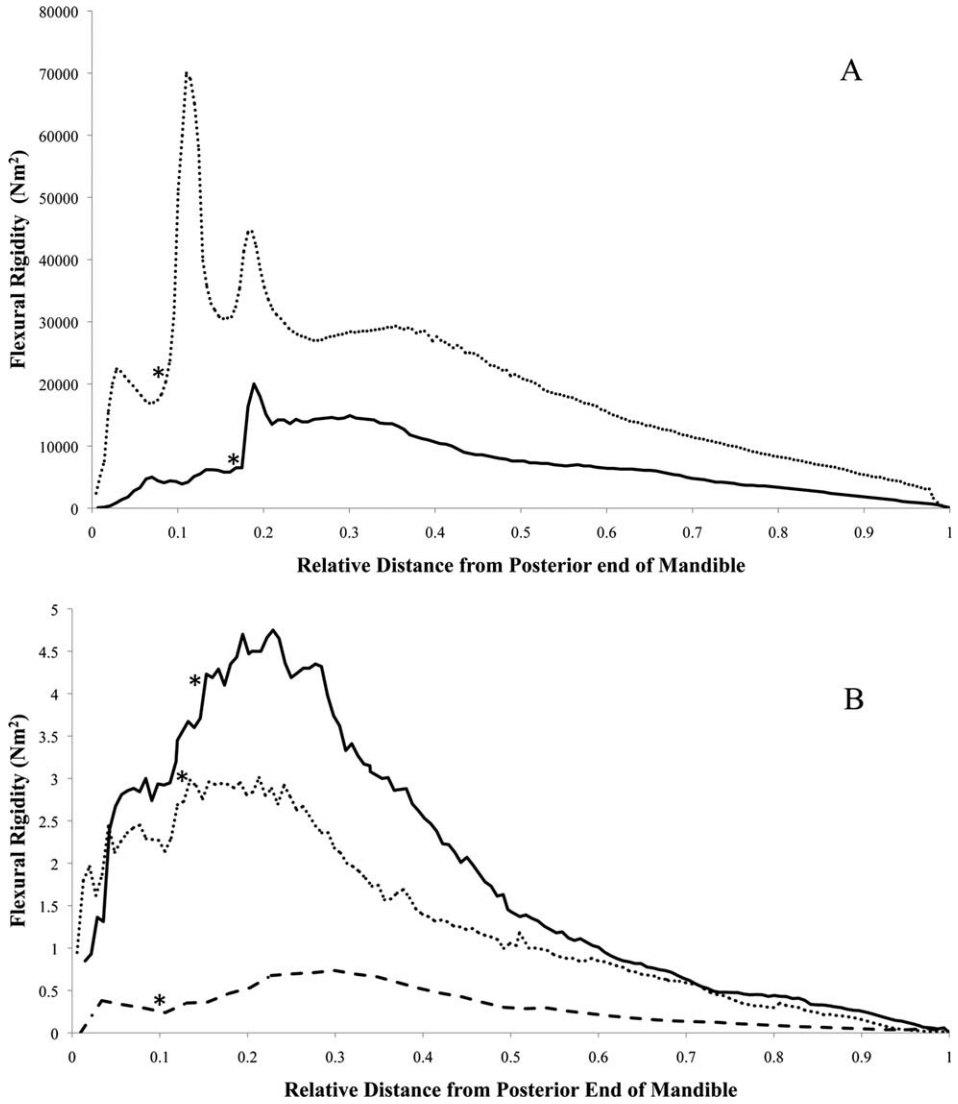

Fig. 3. **A**: Caudorostral flexural rigidity trends along the dorsoventral axis for mandibles of a humpback whale (dotted line) and a minke whale (solid line). Asterisks denote the anterior extent of the TMJ pads. Increasing trends in flexural rigidity from the mandibular symphysis to the anterior extent of the TMJ pads are observed in both rorquals. **B**: Caudorostral flexural rigidity trends along the dorsoventral axis for mandibles of a Brown Pelican (solid line), American White Pelican (dotted line) and Double-crested Cormorant (dashed line). Asterisks denote anterior extent of the posterior jaw musculature. In the white pelican, flexural rigidity increases from the symphysis to the anterior extent of the muscle attachments. Maximal flexural rigidity values are observed at about $x = 0.25$ in the Brown Pelican, just anterior of the muscle attachments. In the Double-crested Cormorant, maximal flexural rigidity is observed at about $x = 0.3$, well anterior of the anterior extent of the posterior jaw musculature.

mediolateral planes. The slope of the best-fit line for the dorsoventral orientation is approximately eight times steeper than that for the mediolateral orientation, meaning that the bone is eight times more resistant to bending dorsoventrally than it is mediolaterally.

Our inflation experiments demonstrated that the pelican pouch is highly distensible and elastic; its mechanical behavior is consistent with that of collagen fiber-reinforced soft tissues such as the dermis of vertebrates and soft-bodied invertebrates (Shadwick, 1992). Biaxial inflation revealed that the pouch tissue is more distensible transversely than longitudinally, thus the bubble inflated as an oblate spheroid: expansion was approximately three times greater in the transverse axis at each pressure. This resulted in two distinct nonlinear stress–strain curves, as seen in Fig. 7. In each axis, the pouch tissue is easily distended at low pressure (= low stress), and becomes much stiffer (indicated by the increasing slope) as the collagen fibers straighten and resist the load at higher pressure. For comparison, a stress–strain curve from VGB of a fin whale is included in Fig. 7. Although this extends to higher strains than the pelican pouch, these data are from a uniaxial test. In this case, as the tissue is stretched transversely it can contract longitudinally, resulting in a greater strain than in a biaxial test where the load is also applied in the longitudinal axis. With this difference in mind, the similarity in mechanical properties of these tissues is apparent.

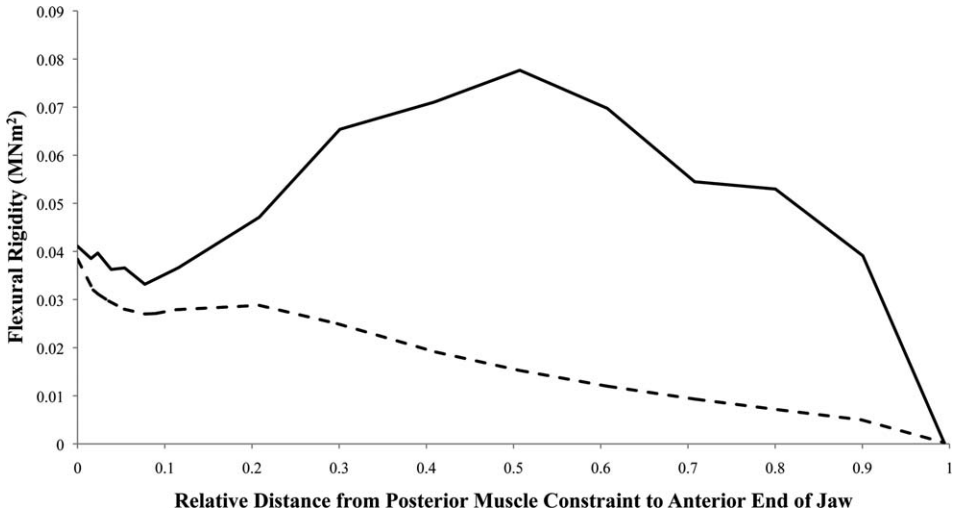

Fig. 4. Comparison of mandibular flexural rigidity trends immediately rostral to the posterior jaw constraint (0 on the *x*-axis), when the contribution of cross-sectional area to flexural rigidity has been eliminated. Solid line = Brown Pelican, dashed line = humpback whale. The humpback jaw exhibits maximal dorsoventral rigidity immediately anterior to the TMJ pads ($x = 0$), where bending stresses are greatest. The difference between the two curves increases anterior to this point as the dorsoventral flexural rigidity of the humpback jaw decreases.

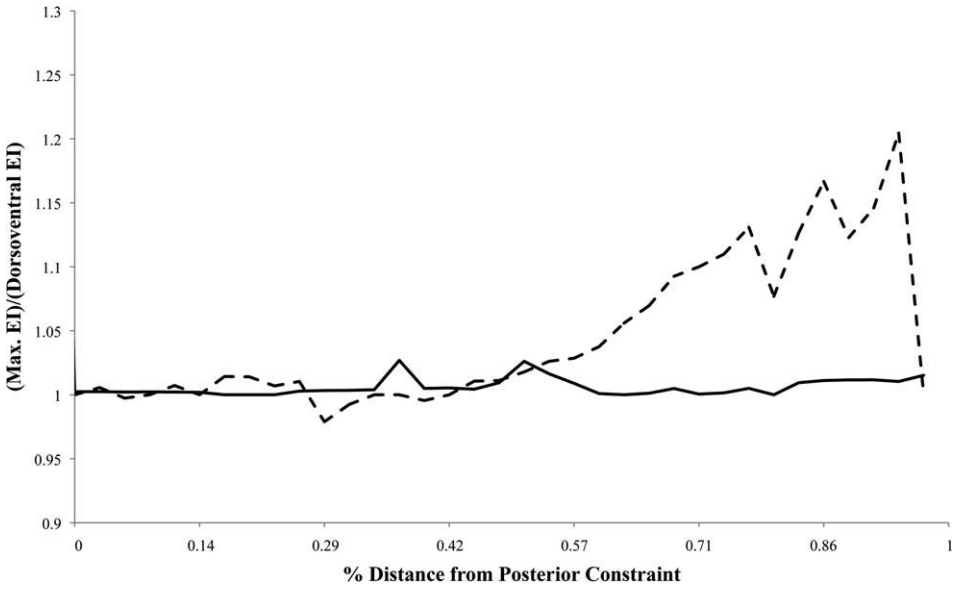

Fig. 5. Ratio between maximum cross-sectional flexural rigidity and dorsoventral flexural rigidity throughout the mandibles of a humpback whale (dashed line) and a Brown Pelican (solid line). The close adherence to 1 in the Brown Pelican indicates that the bone is well designed for bending resistance along its entire length. Values close to 1 are observed at the posterior end of rorqual's mandible, as would be expected since dorsoventral bending stresses are maximal in this region. The rorqual mandible's increasing deviation from 1 in the rostral direction is accompanied by an increasing angular deviation away from the dorsoventral axis. This pattern suggests that other major stresses may act on the anterior portion of the rorqual mandible.

By filling a freshly deceased Brown Pelican's gular pouch with rice to determine its engulfment capacity, and using Archimedes' principle to determine the bird's volume, we found that the bird could increase its volume by approximately 300% during a feeding event. This value is slightly greater than the 250% suggested by Brodie (2001); however, the bird's mass (3.2 kg) and engulfment capacity (ca. 9.6 L) align closely with the average values for Brown Pelicans reported by Schreiber et al. (1975), indicating that our results should be fairly typical of Brown Pelicans in general.

DISCUSSION

Although the more obvious similarities in form and feeding behavior between rorquals and pelicans have been addressed anecdotally (Brodie, 2001), no detailed studies of rorqual–pelican convergence have previously

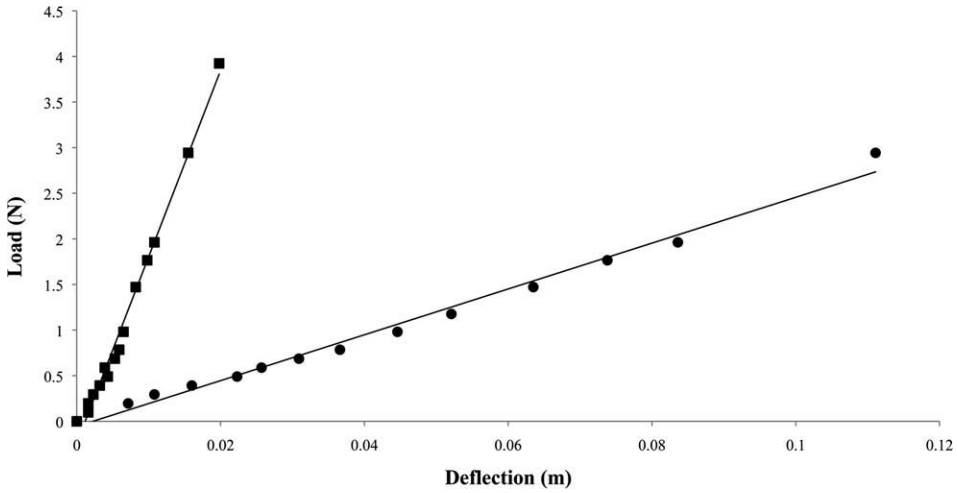

Fig. 6. Load versus deflection plots for the Brown Pelican mandible loaded mediolaterally (circles) and dorsoventrally (squares). Mediolateral line of best fit: $y = 25.123x - 0.0565$; $R_2 = 0.98926$. Dorsoventral line of best fit: $y = 204.23x - 0.2386$; $R_2 = 0.98981$. The slope of these lines represents the object's spring constant (stiffness), and the ratio between the slopes indicates that the bone is approximately eight-times more resistant to bending dorsoventrally than it is mediolaterally.

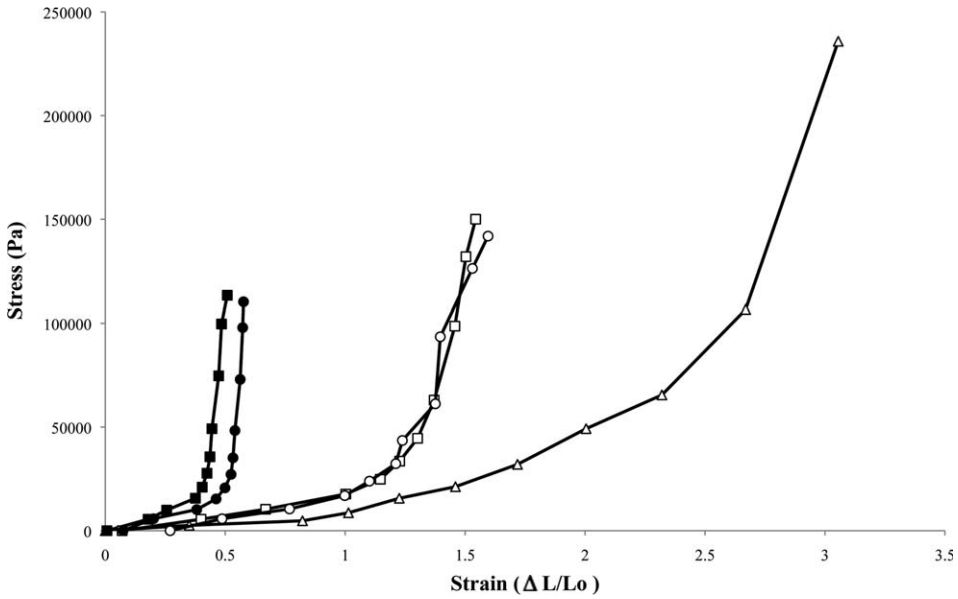

Fig. 7. Representative biaxial stress–strain curves for a piece of pelican pouch, tested by the bubble inflation method (see text). For comparison, a stress–strain curve for the ventral groove blubber of a fin whale (redrawn from Orton and Brodie, 1987) obtained by uniaxial extension is also shown. Triangles = fin whale, closed squares and closed circles = Brown Pelican short axis, open squares and open circles = Brown Pelican long axis. Stress is the tensile force normalized by the initial cross-sectional area, and strain is the proportional change in linear dimension in the transverse and longitudinal axes. The slope of the stress–strain curve at any strain represents stiffness; this increases non-linearly with inflation, with distensibility being about 3 times greater along the transverse axis.

been performed. Unfortunately, prohibitive scanning costs, combined with the size and rarity of cetacean skeletal material, limited both sample sizes and taxon sampling in this study. However, our results suggest that convergence between rorquals and pelicans is deeper than previously recognized: the selective pressures imposed by similar feeding mechanics have resulted in the convergent evolution of an effective jaw design for resisting bending, and of similarly extensible buccal tissue enabling the engulfment of large volumes of water. In the future, detailed comparative studies will shed more light on the convergent evolution of engulfment feeding, and the mechanical adaptations associated with it.

Convergent Flexural Rigidity Trends

A cantilever beam that experiences uniform loading will encounter bending stresses that are maximal at its

fixed end and decrease toward its free end, varying as $(L - x)^2/2L$, where L is the beam length and x is the distance along the beam from the fixed end (Vogel, 2003). The structure experiences no bending stresses where it is constrained. Rorqual and pelican mandibles can be thought of as cantilever beams, with their fixed ends constrained within the craniomandibular joint, and their free ends comprising the mandibular symphysis. During an engulfment-feeding event in these taxa, the extensible tissue comprising the floor of the mouth expands enormously, generating a highly unstreamlined profile. An open mouth moving at high speed underwater generates considerable pressure drag, the same phenomenon that provides resistance to moving an open bag under water (Goldbogen et al., 2007). Additionally, rorquals actively accelerate water in their buccal cavities after a lunge-feeding event, giving rise to "engulfment drag" (Potvin et al., 2009). In both rorquals and pelicans, the elastic floor of the mouth is attached to the ventral surface of the mandibles along their length; therefore, the combined drag forces generated during a feeding event should exert a dorsoventrally oriented bending force distributed along the mandibles, rostral to the craniomandibular joint (Field et al., 2010).

Field et al. (2010) demonstrated that humpback whale mandibles exhibit a density distribution that provides resistance to withstand dorsoventral bending stresses (bone density increasing from the mandibular symphysis posteriorly to the mandibular condyle). In an investigation of jaw architecture in the right whale (*Eubalaena glacialis*), which does not feed by engulfment, Campbell-Malone (2007) discovered the opposite trend in bone density distribution. However, the complexity of determining a nonhomogenous bone's second moment of area prevented Field et al. from investigating the actual flexural rigidity trends throughout rorqual mandibles. Density and cross-sectional area alone, while related to flexural rigidity, may not adequately reflect a bone's resistance to bending. In this study, we found that both rorquals and pelicans exhibit mandibular flexural rigidity distributions that align with the prediction that their mandibles function analogously to a cantilever beam during engulfment feeding. To our knowledge, this investigation represents the first attempt to quantify flexural rigidity distributions throughout vertebrate mandibles using CT data.

Although the maximum dorsoventral flexural rigidity values occur slightly anterior to the craniomandibular joint in Brown Pelicans ($x = 0.2$ on Fig. 3B), Fig. 4 demonstrates that, for its cross-sectional shape, the caudal portion of the Brown Pelican mandible is even more resistant to dorsoventral bending stresses than that of the humpback whale. The Brown Pelican mandible's highest flexural rigidity values are due to a pronounced dorsoventral elongation of the bone; this enlargement clearly would not contribute to the mandible's resistance to breakage due to dorsoventral stresses, because bending stresses would be highest posterior to this region (Vogel, 2003). However, the region corresponding to this area on the Brown Pelican's maxilla is very deep dorsoventrally when compared to that of the American White Pelican. The dorsoventral expansion seen at this point may, therefore, be a design to promote a close seal between the mandible and the maxilla, in order to prevent the escape of prey items from the buccal cavity.

The general flexural rigidity trends through the American White Pelican mandible align with our prediction for cantilever-like bending resistance. However, the magnitude of its dorsoventral flexural rigidity values is markedly lower than those of the similarly sized Brown Pelican mandible, likely reflecting the fact that the bending stresses encountered during surface feeding by American White Pelicans are small in comparison to those encountered by plunge feeding Brown Pelicans.

The flexural rigidity in the dorsoventral axis was also determined for jaws of the Double-crested Cormorant, a seabird that is distantly related to pelicans (Hackett et al., 2008). This analysis revealed a flexural rigidity distribution that is clearly not optimized for dorsoventral bending resistance (Fig. 3B): the maximum flexural rigidity values are located well anterior of the craniomandibular joint (see figure caption), while the bone tapers posteriorly toward the condyles. This results in a low dorsoventral profile at the bone's caudal end that would be weakly resistant to dorsoventral bending. These results give us increased confidence that the dorsoventral flexural rigidity profiles for Brown and American White Pelicans correspond to engulfment feeding behavior.

Interestingly, Fig. 5 suggests that, in addition to the obvious influence of dorsoventral bending, other stresses encountered during feeding may have contributed to the evolution of rorqual mandibular design. While the mandible appears to be optimally suited for bending resistance immediately anterior to the condyles (where such a design would be expected), the anterior portion of the mandible becomes progressively less optimized for dorsoventral bending resistance toward the rostral end, where bending stresses would be at their weakest. It is, therefore, possible that the mandible's morphology in this region reflects the influence of other sources of stress related to lunge feeding, such as torsion. Future finite element modeling may be able to identify alternate stresses encountered by rorqual mandibles during lunge feeding, and should shed light on a possible functional explanation for these observations.

In contrast to the rorqual mandible, Fig. 5 demonstrates that the mandibles of both pelican species show maximal flexural rigidity values in the dorsoventral plane along their entire length. Therefore, while dorsoventral bending likely influences the mandibular design of both rorqual and pelican mandibles, engulfment feeding in pelicans may not result in the same complex stresses affecting the anterior end of lunge feeding rorqual mandibles.

Dual Factors Underlying Mandibular Design in Pelicans

Previous work has examined the mechanical properties of pelican jaws that enable their extraordinary ability to bow outwards in the mediolateral plane (Böker, 1938; Meyers and Myers, 2005). One important specialization enabling this action is the very low mediolateral second moment of area (I) of pelican mandibles (Meyers and Myers, 2005). To ensure that mandibular bowing is controlled and restricted to the mediolateral dimension, bending resistance in the dorsoventral plane may be important. Therefore, the fact that flexural rigidity is much higher in the dorsoventral plane than the mediolateral

plane likely reflects the dual necessities of preventing breakage due to bending stresses while lunge-feeding, and controlling the orientation of mandibular bowing (Bock, 1968). To demonstrate the significant role orientation plays in determining the flexural rigidity of pelican mandibles, Fig. 6 shows load versus deflection plots for a Brown Pelican mandible loaded (A) mediolaterally and (B) dorsoventrally. The difference in slope indicates that the Brown Pelican mandible is approximately eight times more resistant to bending in the dorsoventral orientation than it is in the mediolateral orientation.

Convergent Material Properties of Pelican Gular Pouch Tissue and Rorqual Ventral Groove Blubber

The striking morphological convergence between rorquals and pelicans extends even more deeply than their outward appearance and mandibular flexural rigidity distributions: our inflation experiments reveal that the material properties of the rorqual's extensible VGB and the Brown Pelican's gular pouch are very similar. Although the pelican's pouch is much thinner and smaller than VGB, when the tensile properties are normalized to the sample dimensions (as stress and strain), comparable material properties are revealed (Fig. 7). Both are collagen fiber-reinforced elastic tissues, with sharply nonlinear stress–strain behavior that allows a large volume of water to be captured with a volume limited by high stiffness at high strain. Additionally, these extensible tissues contain an intermediate muscle layer. In rorquals, this muscle layer serves to limit the rate of buccal cavity expansion by accelerating the engulfed water forwards (Potvin et al., 2009). We speculate that the muscle layer may play a similar role in pelicans during engulfment feeding.

Significance of Digital Flexural Rigidity Determination

The inability to effectively obtain flexural rigidity data in a noninvasive manner has hindered studies of functional bone morphology in the past. Determining the flexural rigidity of a bone either demanded full-scale mechanical testing, or the inference of flexural rigidity values from CT data using proxy parameters such as cross-sectional area or bone density (Campbell-Malone, 2007; Field et al., 2010). Not only can full-scale mechanical testing result in damage to rare or valuable museum specimens, but it also cannot distinguish mechanical differences occurring along the bone at different points (Tsukrov et al., 2010). Previous zoological studies attempting to determine flexural rigidity from CT data have been incapable of quantitatively determining I for nonhomogeneous cross-sections, and reliance on densitometry data alone has resulted in loose approximations of flexural rigidity. Therefore, the method presented in this study (BendCT) is significant because it has the potential to nondestructively yield flexural rigidity data, and enables this data to be obtained along the entire length of a bone. We feel that this method has implications for both orthopedic research, as well as future zoological studies in functional bone morphology.

CONCLUSIONS

Our results indicate that the mandibles of rorquals and pelicans exhibit a convergent mechanical design that enables the resistance of dorsoventral bending stresses during engulfment feeding. Further, the similar mechanical properties of rorqual ventral groove blubber and pelican gular pouch tissue may reflect an optimal level of tissue extensibility for this dynamic feeding action. The fact that the Brown Pelican mandible is, for its size, relatively stiffer than the rorqual mandible likely indicates that the bending stresses encountered by the mandibles of diving pelicans are relatively greater than those encountered by rorqual mandibles. Regardless, the mechanical similarities between rorqual and pelican engulfment feeding are clear. The morphological similarities between rorquals and pelicans, which have been demonstrated to extend beyond their external appearance, should qualify rorqual/pelican morphology as a textbook example of convergent evolution between representatives of two distantly related vertebrate classes.

ACKNOWLEDGEMENTS

Sampath Seneviratne provided access to specimens at the University of British Columbia's Cowan Vertebrate Museum. Eddie Kisfaludy kindly provided the Brown Pelican specimen that was used for tests on the gular pouch. Gabor Szathmary, Heather Robertson and Danmei Liu assisted with CT scanning, Regina Campbell-Malone provided QCT expertise, and Wayne Vogl was an enthusiastic source of anatomical knowledge. Scott Gillihan and Michael Murphy of the American Ornithologist's Union graciously permitted the use of the plunge feeding Brown Pelican photo in Fig. 1, and Doug Perrine kindly allowed us to reproduce his spectacular image of a lunge feeding Bryde's whale. Allison Hsiang and Rachel Racicot provided helpful improvements to the manuscript. An NSERC undergraduate student research award to DJF (held at the University of British Columbia) and an NSERC discovery grant to RES funded this research.

LITERATURE CITED

Allen WE. 1923. Fishing activities of the California Brown Pelican. Condor 25:107–108.

Anderson JGT. 1991. Foraging behavior of the American White Pelican (*Pelecanus erythrorhyncos*) in western Nevada. Colonial Waterbirds 14:166–172.

Bock WJ, Kummer B. 1968. The avian mandible as a structural girder. J Biomech 1:89–96.

Böker H. 1938. Die anatomische konstruktion zur erweiterung des unterschnables bei den pelikanen. Anatomischer Anzeiger 87: 294–303.

Brodie PF. 2001. Feeding mechanics of rorquals (*Balenoptera* sp.). In: Mazin J-M, de Buffrenil V, editors. Secondary adaptations of Tetrapods to life in water. Munchen, Germany: Verlag Dr. Friedrich Pfeil. p 345–352.

Burton PJK. 1977. Lower jaw action during prey capture by pelicans. Auk 94:785–786.

Campbell-Malone R. 2007. Biomechanics of north Atlantic right whale bone: mandibular fracture as a fatal endpoint for blunt vessel-whale collision modeling. Doctoral Thesis in Biological Oceanography. Massachusetts Institute of Technology/Woods Hole Oceanographic Institution, Cambridge, MA. p 257.

Charalambides MN, Wanigasooriya L, Williams GJ, Chakrabarti S. 2002. Biaxial deformation of dough using the bubble inflation technique. Rheol Acta 41:532–540.

Field DJ, Campbell-Malone R, Golbogen JA, Shadwick RE. 2010. Quantitative computed tomography of humpback whale (*Megaptera novaeangliae*) mandibles: mechanical implications for rorqual lunge-feeding. Anat Rec 293:1240–1247.

Goldbogen JA, Pyenson ND, Shadwick RE. 2007. Big gulps require high drag for fin whale lunge feeding. Marine Ecol Prog Ser 349:289–301.

Hackett SJ, Kimball RT, Reddy S, Bowie RCK, Braun EL, Braun MJ, Chojnowski JL, Cox WA, Han K-L, Harshman J, Huddleston CJ, Marks BD, Miglia KJ, Moore WS, Sheldon FH, Steadman DW, Witt CC, Yuri T. 2008. A phylogenomic study of birds reveals their evolutionary history. Science 320:1763–1768.

Hong J, Cabe GD, Tedrow JR, Hipp JA, Snyder BD. 2003. Failure of trabecular bone with simulated lytic defects can be predicted non-invasively by structural analysis. J Orthop Res 22: 479–486.

Judin KA. 1961. On mechanism of the jaw in Charadriiformes, Procellariiformes, and some other birds. Trudy Zoological Institute, Leningrad 29:257–302.

Lambertsen RH, Ulrich N, Straley J. 1995. Frontomandibular stay of Balaenopteridae: a mechanism for momentum recapture during feeding. J Mammal 76:877–899.

McSweeney T, Stoskopf MK. 1989. Selected anatomical features of the neck and gular sac of the Brown Pelican (*Peleacnus occidentalis*). J Zoo Anim Med 19:116–121.

Meyers RA, Myers RP. 2005. Mandibular bowing and mineralization in Brown Pelicans. Condor 107:445–449.

Murphy N, Hanley J, McCartin J, Lanigan B, McLoughlin S, Jerrams S, Clauss G, Johannknecht R. 2005. Determining multiaxial fatigue in elastomers using bubble inflation. In: 4th European Conference on Constitutive Models for Rubber (ECCMR), Stockholm.

Orton LS, Brodie PF. 1987. Engulfing mechanics of fin whales. Can J Zool 65:2898–2907.

Owre OT. 1967. Adaptations for locomotion and feeding in the Anhinga and the Double-crested Cormorant. Amer Ornithol Union Ornithol Monogr No. 6, 138 pp.

Potvin J, Goldbogen JA, Shadwick RE. 2009. Passive versus active engulfment: verdict from trajectory simulations of lunge-feeding fin whales *Balaenoptera physalus*. J R Soc Interface. doi: 10.1098/rsif.2008.0492

Reuge N, Schmidt FM, Le Maoult Y, Rachik M, Abbé F. 2001. Elastomer biaxial characterization using bubble inflation technique. I: Experimental investigations. Polym Eng Sci 41:522–531. doi: 10.1002/pen.10749

Rice JC, Cowin SC and Bowman JA. 1988. On the dependence of the elasticity and strength of cancellous bone on apparent density. J Biomech 21:155–168.

Schreiber RW, Woolfenden GE, Curtsinger WE. 1975. Prey capture by the Brown Pelican. Auk 92:649–654.

Shadwick RE. 1992. Soft composites. In: Vincent JFV, editor. Biomechanics—Materials: A practical approach. Oxford: Oxford University Press. p 133–164.

Tsukrov I, DeCew JC, Baldwin K, Campbell-Malone R, Moore MJ. 2009. Mechanics of the right whale mandible: full scale testing and finite element analysis. J Exp Marine Biol Ecol 374:93–103.

Vogel S. 2003. Comparative Biomechanics. Princeton, NJ: Princeton University Press. p 365–373.